LETTER • OPEN ACCESS

Regional climate model projections underestimate future warming due to missing plant physiological CO_2 response

To cite this article: Clemens Schwingshackl *et al* 2019 *Environ. Res. Lett.* **14** 114019

View the article online for updates and enhancements.

Environmental Research Letters

LETTER

CrossMark

Regional climate model projections underestimate future warming due to missing plant physiological CO_2 response

Clemens Schwingshackl[1,2] , Edouard L Davin[1] , Martin Hirschi[1] , Silje Lund Sørland[1] , Richard Wartenburger[1] and Sonia I Seneviratne[1]

[1] Institute for Atmospheric and Climate Science, ETH Zurich, Zurich, Switzerland
[2] Now at Center for International Climate Research (CICERO), Oslo, Norway

E-mail: clemens.schwingshackl@cicero.oslo.no and edouard.davin@env.ethz.ch

Abstract

Many countries rely on regional climate model (RCM) projections to quantify the impacts of climate change and to design their adaptation plans accordingly. In several European regions, RCMs project a smaller temperature increase than global climate models (GCMs), which is hypothesised to be due to discrepant representations of topography, cloud processes, or aerosol forcing in RCMs and GCMs. Additionally, RCMs do generally not consider the vegetation response to elevated atmospheric CO_2 concentrations; a process which is, however, included in most GCMs. Plants adapt to higher CO_2 concentrations by closing their stomata, which can lead to reduced transpiration with concomitant surface warming, in particular, during temperature extremes. Here we show that embedding plant physiological responses to elevated CO_2 concentrations in an RCM leads to significantly higher projected extreme temperatures in Europe. Annual maximum temperatures rise additionally by about 0.6 K (0.1 K in southern, 1.2 K in northern Europe) by 2070–2099, explaining about 67% of the stronger annual maximum temperature increase in GCMs compared to RCMs. Missing plant physiological CO_2 responses thus strongly contribute to the underestimation of temperature trends in RCMs. The need for robust climate change assessments calls for a comprehensive implementation of this process in RCM land surface schemes.

1. Introduction

Increasing atmospheric CO_2 concentrations enhance temperatures on Earth through a stronger absorption of longwave radiation in the atmosphere. In addition to this radiative effect, changing CO_2 concentrations also impact plant physiology (Engineer *et al* 2016): at higher CO_2 concentrations plants can increase the fraction of carbon assimilation to transpiration (i.e. the water-use efficiency) by closing pores ('stomata') that are situated on their leaf surface (Morison 1985, Keenan *et al* 2013). Depending on water availability, these plant physiological CO_2 responses affect the hydrological cycle in different ways. In water-limited regions, higher water-use efficiency can lead to vegetation greening (Donohue *et al* 2013) and a reduction of streamflow (Ukkola *et al* 2016). In regions where water is not limited, however, CO_2-enrichment experiments

find a decrease of transpiration at elevated CO_2 concentrations for various vegetation types (Bernacchi and VanLoocke 2015, Donohue *et al* 2017). By altering water fluxes between the land surface and the atmosphere, plant physiological CO_2 responses do not only influence the hydrological cycle but also the surface energy balance linked to it. In particular, a decrease of (evapo-)transpiration, which can be caused by smaller stomata openings, shifts the partitioning of net radiation towards higher sensible heat fluxes, resulting in increased near-surface air temperatures (Cao *et al* 2010, Seneviratne *et al* 2010). Moreover, reduced evapotranspiration can induce cloud cover reductions, leading to higher temperatures through enhanced incoming shortwave radiation (Skinner *et al* 2018).

Land surface models, which form an integral part of current Earth system models, have incorporated

plant physiology in their evapotranspiration schemes since the 1990s (Sellers *et al* 1997). In fact, several studies using global climate model (GCM) simulations of the Coupled Model Intercomparison Project phase 5 (CMIP5) showed that stomatal adaptation can substantially affect the hydrological cycle (Lemordant *et al* 2018, Hong *et al* 2019) and contribute to the amplification of future heat extremes (Skinner *et al* 2018, Lemordant and Gentine 2019). While most of the GCMs participating in CMIP5 consider plant physiological responses to CO_2 increase (Swann *et al* 2016) and despite the importance of this process, regional climate models (RCMs) generally do not (see references in section 2.1). We hypothesise that this systematic discrepancy might be partly responsible for the fact that RCMs predict a smaller temperature increase than GCMs over several European regions (Kjellström *et al* 2018, Sørland *et al* 2018). Evaluating potential discrepancies between RCMs and GCMs is of high importance, since the local climate information obtained from RCM simulations often constitutes the basis for regional impact and adaptation studies (e.g. Rummukainen 2016, Giorgi 2019).

To quantify how plant physiological CO_2 responses impact climate projections and to assess the extent to which they contribute to the reported temperature differences between RCM and GCM projections in Europe, we employ different sets of regional and global climate model simulations. We first quantify differences in extreme temperature projections between RCMs and GCMs using RCM simulations from 21 RCM–GCM model chains of the EURO-CORDEX ensemble (Jacob *et al* 2014) and the respective simulations from the nine GCMs that are used as boundary conditions for the RCM simulations. Employing the state-of-the-art regional climate model COSMO-CLM^2, which has the option to include plant physiological CO_2 responses, we evaluate the climate effects of introducing stomatal adaptation in an RCM, in order to quantify how much of the GCM–RCM differences can be explained by this process. Finally, we use existing global climate model simulations and observational data to check the validity of the plant physiological CO_2 responses in COSMO-CLM^2. Specifically, we analyse two sets of CMIP5 experiments, in which CO_2 increases by 1% each year, one considering plant physiological CO_2 responses while the other one does not, and observational data from various CO_2-enrichment experiments conducted in forests, grasslands, and agricultural areas.

2. Data and methods

2.1. EURO-CORDEX simulations
To evaluate differences in future climate projections between GCMs and RCMs, regional climate model simulations from the European branch of the Coordinated Downscaling Experiment (EURO-CORDEX; Jacob *et al* 2014) are used. The EURO-CORDEX simulations are performed over Europe for the period 1971–2099. Greenhouse gas concentrations are prescribed as historical trends until 2005, followed by the RCP8.5 scenario (Riahi *et al* 2011). Lateral boundary conditions and sea surface temperatures (SSTs) are provided by a set of GCMs from the CMIP5 ensemble.

The EURO-CORDEX ensemble has been applied by various national agencies to derive information on future regional climate change (Kotlarski *et al* 2014, Brasseur *et al* 2017, Lowe *et al* 2018), serving as basis for the countries' mitigation and adaptation plans. For the Swiss Climate Scenarios CH2018 (CH2018 2018), which provide regional climate projections for Switzerland, the quality of the EURO-CORDEX simulations was assessed and models with obvious issues were excluded from the ensemble (details can be found in the CH2018 report; CH2018 2018). In cases where more than one resolution (either 0.11° or 0.44°) is available for a given model-chain, only the simulation with the higher resolution is used. On the basis of this assessment, the CH2018 scenarios consider 21 GCM–RCM model chains, which we also selected as model ensemble for our study (supplementary figure 1, available online at stacks.iop.org/ERL/14/114019/mmedia). To focus on the question of whether the choice of GCM or RCM simulations changes climate projections over the European domain, we compare the 21 RCM simulations to the simulations of the nine driving GCMs. By limiting our analysis to the driving GCMs we can discriminate any potential effects that would be introduced through an enlargement to the full CMIP5 model ensemble.

According to the respective model descriptions, none of the RCMs but seven out of the nine driving GCMs consider plant physiological CO_2 responses. The 21 GCM–RCM model chains include simulations from seven different RCMs (see supplementary table 1). The land surface models of the RCMs CCLM4-8-17 (using the land surface model TERRA; Doms *et al* 2011), CLMcom5-0-6 (using TERRA; Doms *et al* 2011), HIRHAM5 (using the same land surface model as in ECHAM5; Schulz *et al* 2001, Roeckner *et al* 2003), RegCM4-3 (using BATS; Dickinson *et al* 1993), RACMO22E (using TESSEL; White 2001), REMO2009 (using the same land surface model as in ECHAM4; Roeckner *et al* 1996), and RCA4 (Samuelsson *et al* 2015) calculate plant transpiration without explicit consideration of atmospheric CO_2 concentrations. Thus, increasing atmospheric CO_2 concentrations do not induce plant physiological CO_2 responses in the RCMs.

In contrast to the RCMs, seven out of the nine driving GCMs, which are used as boundary conditions of the EURO-CORDEX domain (see supplementary table 2), consider plant physiological CO_2 responses. These are CanESM2, GFDL-ESM2M, HadGEM2-ES, IPSL-CM5A-MR, MPI-ESM-LR, MIROC5, and Nor-ESM1-M. In contrast, transpiration in CSIRO-Mk3-6-0 and EC-EARTH does not depend on changes of atmospheric CO_2 concentrations (Gordon *et al* 2002,

ECMWF 2007, Gordon *et al* 2010, Hazeleger *et al* 2012).

2.2. COSMO-CLM²

In addition to the EURO-CORDEX simulations we perform simulations with the COSMO-CLM² regional climate model (Davin *et al* 2011, Davin and Seneviratne 2012, Davin *et al* 2016) in order to test the effect of including plant physiological CO_2 responses in an RCM. COSMO-CLM² couples the Consortium for Small-scale Modeling (COSMO) atmospheric model in Climate Mode (so called COSMO-CLM) to the Community Land Model (CLM). Here we use the version 5.0 of COSMO and the version 4.0 of CLM (Oleson *et al* 2010) coupled with OASIS3-MCT. The simulations are performed using the EURO-CORDEX setup as described above over the time period 1949–2099 with a resolution of 0.44°. The global climate model MPI-ESM-LR under RCP8.5 is used as driving GCM. One COSMO-CLM² simulation follows the standard EURO-CORDEX setup (Jacob *et al* 2014) and does not include plant physiological CO_2 responses (hereafter denoted as 'COSMO_NOPHYS'), while the second simulation includes plant physiological responses to rising CO_2 concentrations ('COSMO_PHYS').

In CLM4.0, stomatal conductance is based on the Ball–Berry model (Oleson *et al* 2010), which allows stomatal conductance to adjust to CO_2 concentrations. In COSMO_NOPHYS the CO_2 concentration in the Ball–Berry equation is kept constant (at a level of 367 ppm), whereas in COSMO_PHYS the CO_2 concentration used in the Ball–Berry equation increases according to the RCP8.5 scenario.

2.3. CMIP5 1%CO_2 simulations

To quantify the effects of plant physiological CO_2 responses in CMIP5 models we use simulations, in which CO_2 increases by 1% each year ('1pctCO2', denoted here as 'CMIP5_PHYS'). These simulations can be compared to the 'esmFdbk1' (denoted as 'CMIP5_NOPHYS') simulations, in which CO_2 in the atmosphere also increases by 1% each year, but the CO_2 concentrations used for calculating vegetation processes and the carbon cycle stay constant at pre-industrial levels throughout the whole simulation period. We use eight different climate models, which provide the necessary 1pctCO2 and esmFdbk1 simulations (see supplementary table 3). We exclude GFDL-ESM2M, in which CO_2 concentrations only increase until year 70 of the 1pctCO2 and esmFdbk1 simulations and do thus not reach the CO_2 levels, which are necessary to compare to the years 2070–2099 in the RCP8.5 scenario (see below). The evolution of CO_2 concentrations in BCC-CSM1-1 and CanESM2 is taken from the data provided in the CMIP5 archive. For the other models a 1% increase per year is assumed starting from 284.7 ppm for NorESM1-ME, CESM1-BGC, MPI-ESM-LR, IPSL-CM5A-LR, and

IPSL-CM5A-MR and from 286.3 ppm for HadGEM2 (according to the simulation setup as described by the respective modelling groups). Since daily maximum temperature data from NorESM1-ME and IPSL-CM5A-MR for the esmFdbk1 simulations are not fully available, these models are not considered in the CMIP5 ensemble for the analysis of annual maximum temperatures (TXx).
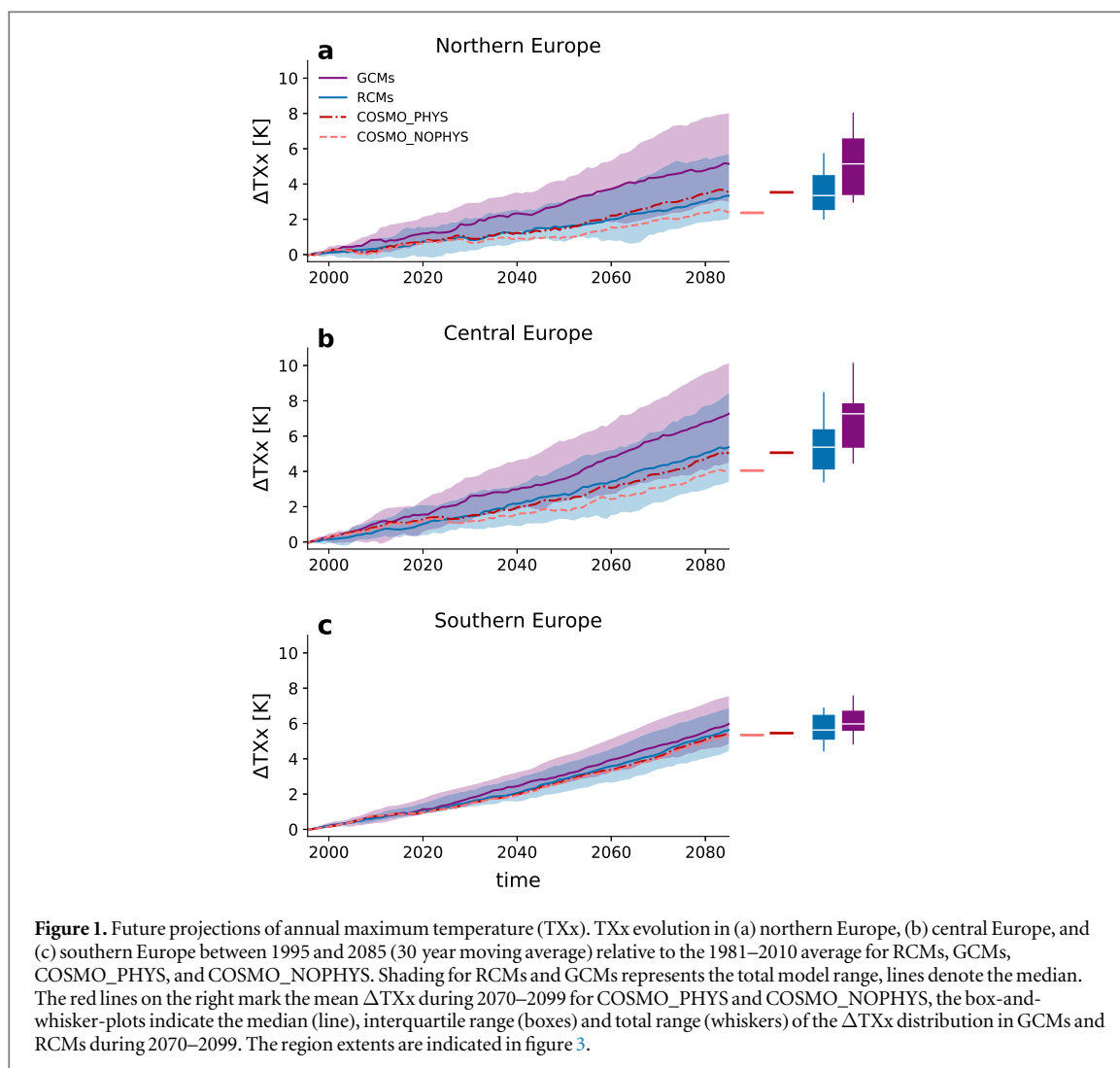
To compare the 1pctCO2 and esmFdbk1 simulations to the RCP8.5 scenario (which is used for the RCM, GCM, and COSMO-CLM² simulations) we select those simulation years in the 1pctCO2 and esmFdbk1 simulations, in which atmospheric CO_2 concentrations are in the same range as in the historical and RCP8.5 scenarios during the analysed time periods 1981–2010 and 2070–2099. The respective CO_2 concentration ranges are 339.7–389.3 ppm for 1981–2010 and 677.1–926.7 ppm for 2070–2099. Since the scenario setup of 1pctCO2 and esmFdbk1 is different than the historical and RCP8.5 pathways, the absolute changes of climate variables in 1pctCO2 and esmFdbk1 are not directly comparable to the changes in the RCP8.5 simulations. However, the difference between the 1pctCO2 and esmFdbk1 simulations provides a direct estimate of the plant physiological CO_2 effects on climate and can thus also be compared to differences between model simulations with and without plant physiological CO_2 responses in the historical and RCP8.5 scenarios.

2.4. Observations

CO_2-enrichment experiments were conducted on a wide variety of land cover types (Bernacchi and VanLoocke 2015, Donohue *et al* 2017). Here we use experiments, for which evapotranspiration measurements over plots with both ambient and elevated CO_2 concentrations were performed. Moreover, we only use outdoor measurements with open chambers, as closed or indoor systems do not represent realistic turbulent outdoor conditions. All used observations and the respective publications from which they are taken are listed in supplementary table 4.

2.5. Study region

In this study, the effects of plant physiological CO_2 responses in Europe are examined. To analyse the effects in different European climate regimes, we subdivide the European domain into the three study regions northern, central, and southern Europe (see figure 3 for their extents), which correspond to the European regions defined in the Special Report on Extremes (SREX; Seneviratne *et al* 2012). Regional averages over the three study regions are calculated as area-weighted mean using the original grid resolution (individually for each RCM, GCM, and CMIP5 model) and considering each pixel's land fraction.

Figure 1. Future projections of annual maximum temperature (TXx). TXx evolution in (a) northern Europe, (b) central Europe, and (c) southern Europe between 1995 and 2085 (30 year moving average) relative to the 1981–2010 average for RCMs, GCMs, COSMO_PHYS, and COSMO_NOPHYS. Shading for RCMs and GCMs represents the total model range, lines denote the median. The red lines on the right mark the mean ΔTXx during 2070–2099 for COSMO_PHYS and COSMO_NOPHYS, the box-and-whisker-plots indicate the median (line), interquartile range (boxes) and total range (whiskers) of the ΔTXx distribution in GCMs and RCMs during 2070–2099. The region extents are indicated in figure 3.

3. Results

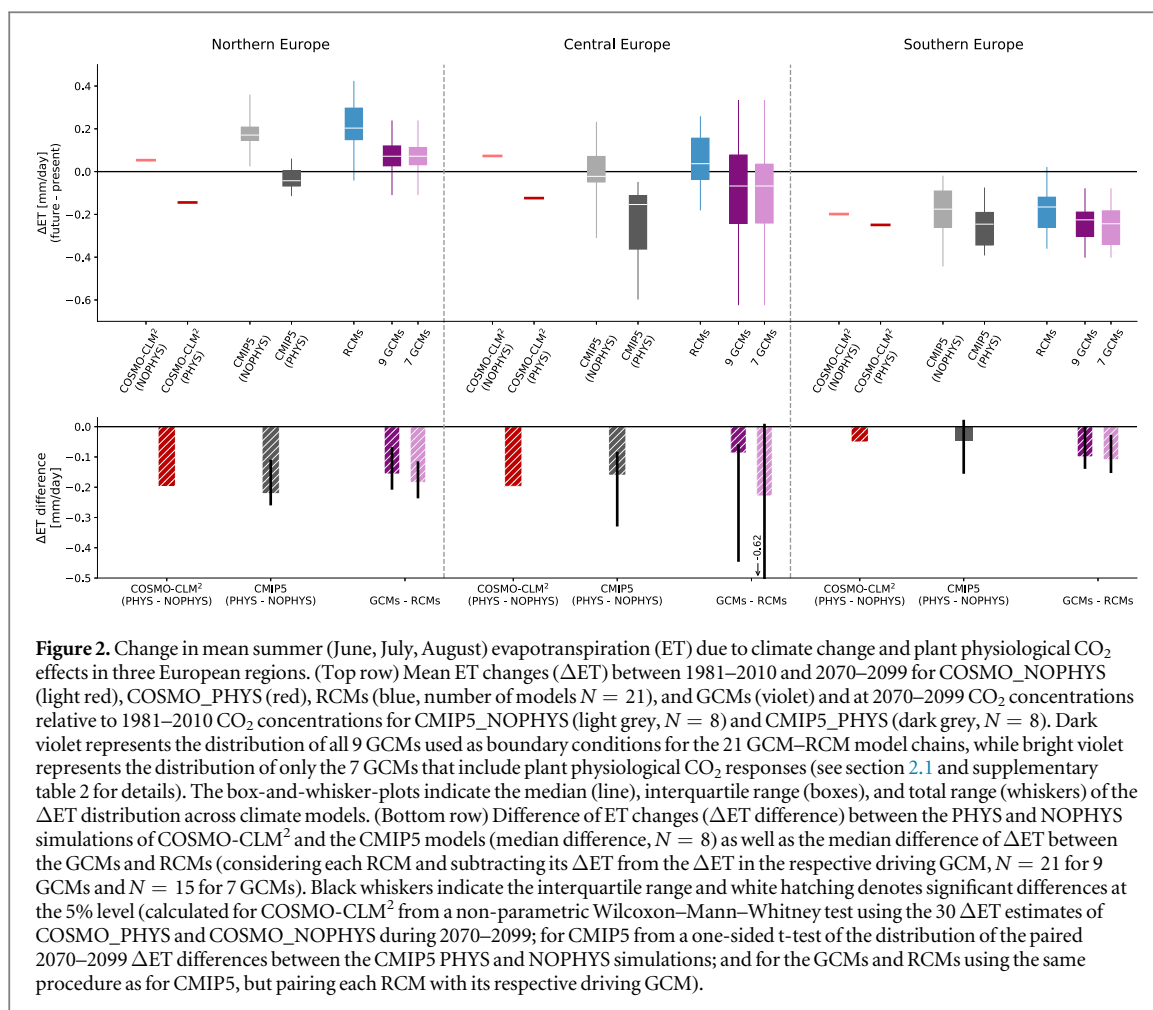### 3.1. Amplified extreme temperature increase in GCMs compared to RCMs

The driving GCMs of the considered EURO-CORDEX model chains exhibit an amplified future increase of the annual maximum temperature (TXx) compared to the RCMs (violet and blue shadings in figure 1). The TXx amplification is strongest in central and northern Europe but only small in southern Europe. Additionally, the inter-model spread in both RCMs and GCMs is large in central and northern Europe but narrower in southern Europe. The amplified TXx increase in GCMs in central and northern Europe is in agreement with the expectation that plant physiological CO_2 effects on temperature are strongest in regions, which are not water limited (Skinner *et al* 2018).

Consistent with the amplified TXx increase in GCMs, COSMO_PHYS exhibits a stronger TXx increase compared to COSMO_NOPHYS in central and northern Europe, while in southern Europe the difference is only small (figure 1). According to the difference between COSMO_PHYS and COSMO_NOPHYS, the contribution of plant physiological

responses to the stronger TXx increase in GCMs compared to RCMs is around 81% in northern and 73% in central Europe (contribution to the median increase of all paired 21 GCM–RCM combinations). Note that the TXx signal in COSMO-CLM² is on the lower side compared to the RCM ensemble. We anticipate that this is not connected to the CLM land surface scheme, but more likely due to the fact that the driving GCM (MPI-ESM-LR, see section 2.2) used to force COSMO-CLM² shows a lower temperature change signal than many of the other GCMs in the EURO-CORDEX ensemble (Sørland *et al* 2018, Kjellström *et al* 2018).

3.2. Evapotranspiration reduction due to plant physiological CO_2 responses

The amplified TXx increase in COSMO_PHYS can be attributed to the fact that smaller stomata openings affect evapotranspiration (ET). Future ET in COSMO_PHYS is significantly reduced compared to COSMO_NOPHYS (figure 2). Especially in central and northern Europe the ET reduction is substantial (−0.20 mm/day), while in southern Europe it is only small (−0.05 mm/day). The ET difference between

Figure 2. Change in mean summer (June, July, August) evapotranspiration (ET) due to climate change and plant physiological CO_2 effects in three European regions. (Top row) Mean ET changes (ΔET) between 1981–2010 and 2070–2099 for COSMO_NOPHYS (light red), COSMO_PHYS (red), RCMs (blue, number of models $N = 21$), and GCMs (violet) and at 2070–2099 CO_2 concentrations relative to 1981–2010 CO_2 concentrations for CMIP5_NOPHYS (light grey, $N = 8$) and CMIP5_PHYS (dark grey, $N = 8$). Dark violet represents the distribution of all 9 GCMs used as boundary conditions for the 21 GCM–RCM model chains, while bright violet represents the distribution of only the 7 GCMs that include plant physiological CO_2 responses (see section 2.1 and supplementary table 2 for details). The box-and-whisker-plots indicate the median (line), interquartile range (boxes), and total range (whiskers) of the ΔET distribution across climate models. (Bottom row) Difference of ET changes (ΔET difference) between the PHYS and NOPHYS simulations of COSMO-CLM^2 and the CMIP5 models (median difference, $N = 8$) as well as the median difference of ΔET between the GCMs and RCMs (considering each RCM and subtracting its ΔET from the ΔET in the respective driving GCM, $N = 21$ for 9 GCMs and $N = 15$ for 7 GCMs). Black whiskers indicate the interquartile range and white hatching denotes significant differences at the 5% level (calculated for COSMO-CLM^2 from a non-parametric Wilcoxon–Mann–Whitney test using the 30 ΔET estimates of COSMO_PHYS and COSMO_NOPHYS during 2070–2099; for CMIP5 from a one-sided t-test of the distribution of the paired 2070–2099 ΔET differences between the CMIP5 PHYS and NOPHYS simulations; and for the GCMs and RCMs using the same procedure as for CMIP5, but pairing each RCM with its respective driving GCM).
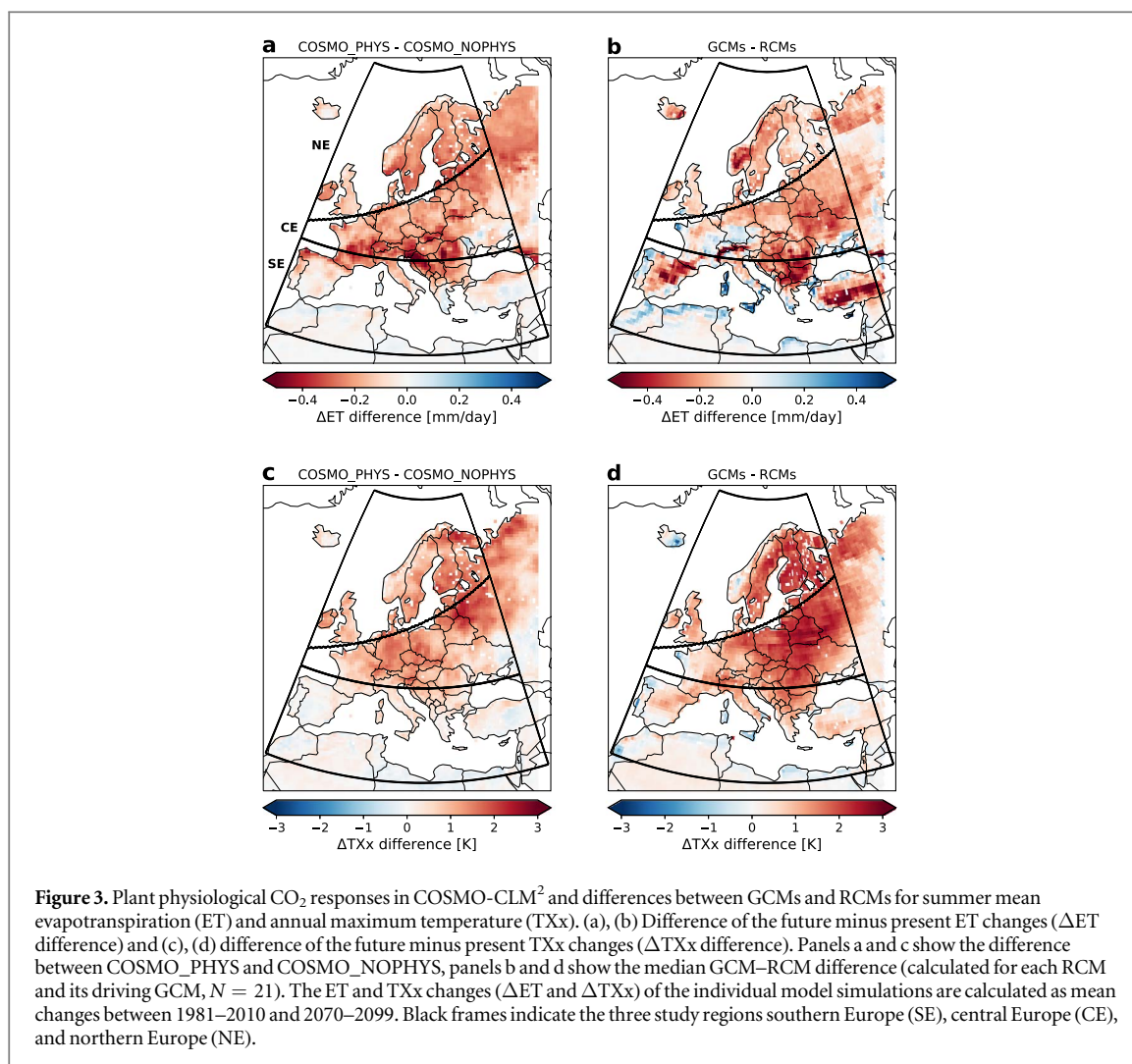
COSMO_PHYS and COSMO_NOPHYS is composed by a substantial reduction in transpiration and a slight increase in bare soil evaporation (supplementary figure 2). The evaporation increase is likely a direct effect of the lower transpiration, which leaves more water in the soil for evaporation. Although the two effects compensate in some regions (particularly in southern and eastern Europe), the dominating signal over central and northern Europe is a considerable decrease of ET (figure 2).

The ET reduction in COSMO_PHYS agrees well with estimates from the dedicated CMIP5 simulations, which aim at quantifying climate effects of plant physiological CO_2 responses (see section 2.3). The median ET reduction due to plant physiological responses in the CMIP5 models (CMIP5_PHYS minus CMIP5_NOPHYS) is similar to the reduction in COSMO-CLM^2 in northern, southern and, a bit less pronounced, in central Europe (figure 2). The ET effect in COSMO-CLM^2 can also be compared to ET measurements from CO_2-enrichment experiments, in which plants are exposed to elevated CO_2 concentrations. The ET sensitivity to atmospheric CO_2 increase in COSMO-CLM^2 (ranging from -1.1%/100 ppm to -2.8%/100 ppm) agrees well with median estimates from various experiments in grasslands (-2.6%/100 ppm, number of observations $N = 7$), crops (-2.8%/100 ppm, $N = 19$), and forests (-1.0%/

100 ppm, $N = 24$), as shown in supplementary figure 3. The ET reduction induced by plant physiological CO_2 responses in COSMO-CLM^2 is thus well in line with both the CMIP5 simulations on plant physiological forcing and the observation-based estimates.

Consistent with plant physiological responses, the nine driving GCMs of the 21 GCM–RCM model chains generally project a reduced ET change compared to RCMs at the end of the 21st century (figure 2). The difference between GCMs and RCMs is largest in northern Europe, where also COSMO-CLM^2 and the CMIP5 models show strong ET reductions due to plant physiological effects, and relatively small in southern Europe. In central Europe, the median GCM–RCM difference is smaller than in northern Europe, but the uncertainty is high and the distribution strongly skewed towards negative values. The ET difference between GCMs and RCMs, displayed in figure 2, is calculated across all 21 GCM–RCM combinations (pairing each RCM with its respective driving GCM), including all GCMs that consider plant physiological CO_2 responses as well as the two GCMs that do not (EC-EARTH and CSIRO-Mk3.6.0). When only considering the 15 GCM–RCM model chains driven by the seven GCMs that include plant physiological CO_2 responses, ET reductions in northern and southern Europe remain robust, but get more pronounced

Figure 3. Plant physiological CO_2 responses in COSMO-CLM^2 and differences between GCMs and RCMs for summer mean evapotranspiration (ET) and annual maximum temperature (TXx). (a), (b) Difference of the future minus present ET changes (ΔET difference) and (c), (d) difference of the future minus present TXx changes (ΔTXx difference). Panels a and c show the difference between COSMO_PHYS and COSMO_NOPHYS, panels b and d show the median GCM–RCM difference (calculated for each RCM and its driving GCM, $N = 21$). The ET and TXx changes (ΔET and ΔTXx) of the individual model simulations are calculated as mean changes between 1981–2010 and 2070–2099. Black frames indicate the three study regions southern Europe (SE), central Europe (CE), and northern Europe (NE).

in central Europe compared to the full ensemble (figure 2).

Both the ET reductions caused by plant physiological CO_2 responses and the ET difference between RCMs and GCMs reveal a north–south gradient with strong ET reductions in northern and small decreases in southern Europe, suggesting that a large part of the ET difference between GCMs and RCMs can be explained by plant physiological responses. The respective ET reductions are also consistent with the amplified TXx increase in GCMs compared to RCMs in northern and central Europe (figure 1), indicating that a considerable percentage of the TXx difference between GCMs and RCMs is indeed due to plant physiological CO_2 responses.

Besides extreme temperatures, plant physiological responses also affect mean temperatures, albeit to a smaller degree (supplementary figure 4). Land temperatures averaged over the European domain are about 0.38 K higher during summer (June, July, August) in COSMO_PHYS than COSMO_NOPHYS and mean annual temperatures are elevated by about 0.15 K. The pronounced seasonal cycle of the plant physiological CO_2 effects on ET and temperature (supplementary figure 5) reflects their importance during the vegetation period. Subtracting the temperature effect stemming from plant physiological responses (estimated by COSMO-CLM^2) from the temperature bias between GCMs and RCMs, which also shows a pronounced seasonal cycle, yields a much more uniform temperature difference in the course of the year (supplementary figure 5). Averaged over the European domain the remaining bias between GCMs and RCMs is about 0.25 K.

3.3. Geographical patterns
The geographical patterns of the ET and TXx differences between COSMO_PHYS and COSMO_NOPHYS and between the GCMs and RCMs are shown in figure 3. The GCM and RCM data are interpolated to 0.5° using conservative remapping before calculating the difference. In COSMO-CLM^2 the ET reduction due to plant physiological CO_2 responses is high almost everywhere in central and northern Europe. The strongest effects occur in a band that spans from southern France to the Black Sea. The ET differences between GCMs and RCMs generally agree with this pattern (pattern correlation of 0.37; Spearman's rank correlation, $p < 0.001$; all datasets regridded to 0.5°)

and also reveal high values in eastern and northern Europe. Over topographically complex terrain (such as the Pyrenees, the Alps, Anatolia, or the Scandinavian Mountains) the ET differences between GCMs and RCMs are especially pronounced, which might be due to the better spatial resolution of RCMs compared to GCMs rather than to plant physiological CO_2 responses.

The TXx patterns generally follow the patterns of decreased ET, with high values occurring especially in central and eastern to northeastern Europe. While ET is more connected to stationary vegetation processes, for the occurrence of TXx also air advection plays a role. Consequently, the TXx patterns are more widespread with respect to the ET patterns. The high pattern correlation of 0.78 (Spearman's rank correlation, $p<0.001$) between the TXx maps of COSMO-CLM^2 and the GCM–RCM maps highlights again the close connection between the plant physiological effects on TXx estimated with COSMO-CLM^2 and the TXx difference between GCMs and RCMs.

4. Discussion

The amplified TXx increase in COSMO_PHYS compared to COSMO_NOPHYS can be attributed to the stomatal response to elevated CO_2 concentrations in COSMO_PHYS. Smaller stomata openings lead to ET reductions, which affect atmospheric temperatures in two ways. Reduced ET induces an increase of the fraction of net radiation that is converted to sensible heat flux, causing a stronger heating of near-surface air and affecting, in particular, extreme temperatures (Miralles *et al* 2014, Perkins 2015). Moreover, reduced ET can induce cloud cover reductions, which leads to higher temperatures through enhanced incoming shortwave radiation. The combined effects lead to pronounced amplifications of TXx in central and northern Europe.

Besides plant physiological CO_2 responses, GCMs and RCMs also exhibit differences related to the representation of topography, cloud processes, and aerosol forcing (Giorgi and Gao 2018, Sørland *et al* 2018). In particular, the discrepant aerosol trends have recently been discussed as possible cause for divergent GCM and RCM climate projections (Nabat *et al* 2016, Bartók *et al* 2017, Giorgi and Gao 2018, Sørland *et al* 2018). The emission scenario RCP8.5 used in the GCM, RCM, and COSMO-CLM^2 simulations project a strong aerosol reduction over Europe until 2100 (Riahi *et al* 2011, IPCC 2013). While all GCMs incorporate this trend, aerosols in the RCMs used in this study (including COSMO-CLM^2) are usually prescribed as climatological values without any long-term trends (Giorgi and Gao 2018). Especially over Europe, reduced aerosol loads contribute an important fraction to the future radiative forcing in GCMs (Westervelt *et al* 2015) but not in RCMs (Giorgi and Gao 2018). A model study

with one RCM estimated a temperature increase of 0.3 K over Europe when using RCP8.5 aerosol trends instead of constant aerosol concentrations (Nabat *et al* 2016), which is consistent with the 0.25 K temperature bias not explained by plant physiological CO_2 responses (see section 3.2). While aerosol radiative forcing is projected to increase mostly in the Mediterranean area and central Europe (IPCC 2013), the ET and TXx differences between GCMs and RCMs are highest in central and northern Europe but only small in southern Europe. This pattern agrees much better with the expected effects of plant physiological CO_2 responses (see figure 2) than with aerosol effects, suggesting that plant physiology is likely the largest contributor to the TXx amplification in GCMs compared to RCMs in large parts of Europe.

The high ET uncertainty of the GCM–RCM differences in central Europe (figure 2) are mainly due to a large spread of GCMs (Supplementary figure 6). In contrast, the spread of the RCMs driven by the same GCM is much smaller and thus contributes only a small share to the total model spread. Consequently, the estimated ET reductions in central Europe strongly depend on the choice of GCMs considered in the GCM–RCM model chains. This large uncertainty in the estimated ET reductions in central Europe is likely connected to the divergent ET trend projections by GCMs in this region (Vogel *et al* 2018). In contrast, the different ET reduction estimates agree well in northern and southern Europe, which gives confidence in the robustness of the estimated plant physiological effect on ET in these regions. Especially in central Europe, also the TXx estimates depend on the number of GCM–RCM model chains considered (supplementary figure 7). Higher TXx values are related with stronger ET reductions and vice versa (figure 2), revealing the close correlation between ET and TXx. This correlation highlights the importance of ET for TXx projections in central Europe and clearly points out that ET reductions caused by plant CO_2 responses can considerably affect TXx.

The geographical patterns of the ET differences (figures 2 and 3) are in line with the expected ET reductions in non-water-limited regions such as central and northern Europe (Donohue *et al* 2013, Bernacchi and VanLoocke 2015), while ET decreases are lower or negligible in water-limited regions like southern Europe (Fatichi *et al* 2016, Skinner *et al* 2018). Summer transpiration in southern Europe is already low in the present (supplementary figure 2) and all model sets (COSMO-CLM^2, CMIP5, RCMs, and GCMs) project a net ET decrease in the future (see figure 2, upper right panel). Including plant physiological CO_2 effects in COSMO-CLM^2 and CMIP5 only leads to a slight additional ET reduction, suggesting that water limitations rather than stomatal effects are the dominating factor for future ET evolution in southern Europe.

In water-limited regions, water savings due to reduced ET can also extend the growing season (Reyes-Fox *et al* 2014). Moreover, increasing CO_2 generally leads to an ET decrease in undisturbed vegetation, while it induces greening in disturbed (not full-grown or damaged) vegetation, which counteracts the ET reduction and can even cause an enhancement of ET (Donohue *et al* 2017). COSMO-CLM^2, which is used in this study, does not consider vegetation dynamics. Instead, leaf area index is prescribed as climatology with no long-term changes throughout the simulation period and the effects of vegetation disturbance and growing season changes are thus not considered. While vegetation disturbance effects might impact the results of this study, possible extensions of the growing season should be less important as TXx typically occurs during summer.

5. Conclusions

Plant physiological CO_2 responses have the potential to substantially impact the hydrological cycle (Cao *et al* 2010, Hong *et al* 2019, Lemordant *et al* 2018) and amplify future extreme temperatures (Skinner *et al* 2018, Lemordant and Gentine 2019). While most of the GCMs contributing to CMIP5 consider plant physiological CO_2 responses, RCMs used in the EURO-CORDEX simulations generally do not. Here we investigate to which extent this discrepancy is responsible for the stronger TXx increase in GCMs compared to RCMs in large parts of Europe by performing dedicated simulations with the regional climate model COSMO-CLM^2. Including plant physiological CO_2 responses in COSMO-CLM^2 leads to pronounced ET decreases in central and northern Europe, but only small ET reductions in southern Europe (figure 2). The patterns and amount of ET reduction agree well with results from CMIP5 simulations, which also aim at quantifying impacts of plant physiological CO_2 responses. Moreover, the ET reduction patterns of COSMO-CLM^2 fit with the expectations that plant physiological CO_2 responses cause ET reductions in regions with abundant water availability but not in water-limited regions (figure 3; Bernacchi and VanLoocke 2015, Donohue *et al* 2013, 2017, Ukkola *et al* 2016). While the ET reductions in northern and southern Europe caused by stomatal adaptation are robust across models, the effects in central Europe are more uncertain, ranging from small to potentially very large ET decreases (figure 2). The high uncertainty stems from ET reductions being very sensitive to the selection of GCMs in central Europe and thus mainly reflects the divergent ET trend projections by GCMs in this region (Vogel *et al* 2018).

Including plant physiological CO_2 responses in COSMO-CLM^2 leads to pronounced TXx increases in central and northern Europe (figure 1). The results suggest that on average about 67% of the additional TXx increase in GCMs compared to RCMs in Europe are due to plant physiological CO_2 effects. ET and TXx are closely coupled in all regions, with small TXx increases occurring where ET reduces only slightly, but high TXx increases where ET reductions are pronounced (figure 2 and supplementary figure 7). While divergent aerosol trends in GCMs and RCMs have been discussed as potential reason for discrepancies in temperature projections between GCMs and RCMs (Nabat *et al* 2016, Bartók *et al* 2017, Giorgi and Gao 2018, Sørland *et al* 2018), plant physiological CO_2 responses seem to additionally play a very important role for future extreme temperature evolution in Europe.

Our study highlights the need to include plant physiological CO_2 responses in other RCMs in order to provide regional climate projections that are physically consistent with the driving GCMs. Given the importance of RCM projections in providing information for impact studies and the design of adaptation plans (Gutowski *et al* 2016), it is crucial that RCMs reflect the most recent advances in our understanding of land–atmosphere interactions.

Data availability

COSMO-CLM^2 data and the RCM and GCM data used to create the plots are made available on the ETH Research Collection under doi:10.3929/ethz-b-000360999. CMIP5 data are available from https://esgf-node.llnl.gov/search/cmip5 and EURO-CORDEX data from https://esgf-data.dkrz.de/search/cordex-dkrz.

ORCID iDs

Clemens Schwingshackl ⓘ https://orcid.org/0000-0003-4048-3011
Edouard L Davin ⓘ https://orcid.org/0000-0003-3322-9330
Martin Hirschi ⓘ https://orcid.org/0000-0001-9154-756X
Silje Lund Sørland ⓘ https://orcid.org/0000-0002-1537-0851
Richard Wartenburger ⓘ https://orcid.org/0000-0003-4470-5080
Sonia I Seneviratne ⓘ https://orcid.org/0000-0001-9528-2917

References

Bartók B *et al* 2017 Projected changes in surface solar radiation in CMIP5 global climate models and in EURO-CORDEX regional climate models for Europe *Clim. Dyn.* **49** 2665–83

Bernacchi C J and VanLoocke A 2015 Terrestrial ecosystems in a changing environment: a dominant role for water *Annu. Rev. Plant Biol.* **66** 599–622

Brasseur G P, Jacob D and Schuck-Zöller S 2017 *Klimawandel in Deutschland: Entwicklung, Folgen, Risiken und Perspektiven* (Berlin: Springer) (https://doi.org/10.1007/978-3-662-50397-3)

Cao L, Bala G, Caldeira K, Nemani R and Ban-Weiss G 2010 Importance of carbon dioxide physiological forcing to future climate change *Proc. Natl Acad. Sci.* **107** 9513–8

CH2018 2018 Climate scenarios for Switzerland *Tech. Rep.* (Zurich: National Centre for Climate Services)

Davin E L, Maisonnave E and Seneviratne S I 2016 Is land surface processes representation a possible weak link in current regional climate models? *Environ. Res. Lett.* **11** 074027

Davin E L and Seneviratne S I 2012 Role of land surface processes and diffuse/direct radiation partitioning in simulating the European climate *Biogeosciences* **9** 1695–707

Davin E L, Stöckli R, Jaeger E B, Levis S and Seneviratne S I 2011 COSMO-CLM^2: a new version of the COSMO-CLM model coupled to the Community Land Model *Clim. Dyn.* **37** 1889–907

Dickinson R E, Henderson-Sellers A and Kennedy J 1993 Biosphere-atmosphere transfer scheme (BATS) version 1e as coupled to the NCAR community climate model *Tech. Rep.* NCAR/TN-387+STR NCAR

Doms G *et al* 2011 A description of the nonhydrostatic regional COSMO model. Part II: physical parameterization Deutscher Wetterdienst, Offenbach, Germany (http://cosmo-model.org/content/model/documentation/core/cosmoPhysParamtr.pdf)

Donohue R J, Roderick M L, McVicar T R and Farquhar G D 2013 Impact of CO_2 fertilization on maximum foliage cover across the globe's warm, arid environments *Geophys. Res. Lett.* **40** 3031–5

Donohue R J, Roderick M L, McVicar T R and Yang Y 2017 A simple hypothesis of how leaf and canopy-level transpiration and assimilation respond to elevated CO_2 reveals distinct response patterns between disturbed and undisturbed vegetation *J. Geophys. Res.: Biogeosci.* **122** 168–84

ECMWF 2007 IFS documentation - CY31R1 *Tech. Rep., Part IV: Physical Processes* (www.ecmwf.int/node/9221)

Engineer C B, Hashimoto-Sugimoto M, Negi J, Israelsson-Nordström M, Azoulay-Shemer T, Rappel W-J, Iba K and Schroeder J I 2016 CO_2 sensing and CO_2 regulation of stomatal conductance: advances and open questions *Trends Plant Sci.* **21** 16–30

Fatichi S, Leuzinger S, Paschalis A, Langley J A, Donnellan Barraclough A and Hovenden M J 2016 Partitioning direct and indirect effects reveals the response of water-limited ecosystems to elevated CO_2 *Proc. Natl Acad. Sci.* **113** 12757–62

Giorgi F 2019 Thirty years of regional climate modeling: Where are we and where are we going next? *J. Geophys. Res.: Atmos.* **124** 5696–723

Giorgi F and Gao X-J 2018 Regional earth system modeling: review and future directions *Atmos. Ocean. Sci. Lett.* **11** 189–97

Gordon H 2002 The CSIRO Mk3 climate system model *Tech. Rep.* 60 CSIRO

Gordon H B, O'Farrell S, Collier M, Dix M, Rotstayn L, Kowalczyk E, Hirst T and Watterson I 2010 The CSIRO Mk3.5 climate model *CAWCR Technical Report* 021 CSIRO and Bureau of Meteorology

Gutowski W J Jr *et al* 2016 WCRP COordinated Regional Downscaling EXperiment (CORDEX): a diagnostic MIP for CMIP6 *Geosci. Model Dev.* **9** 4087–95

Hazeleger W *et al* 2012 EC-Earth V2.2: description and validation of a new seamless earth system prediction model *Clim. Dyn.* **39** 2611–29

Hong T, Dong W, Ji D, Dai T, Yang S and Wei T 2019 The response of vegetation to rising CO_2 concentrations plays an important role in future changes in the hydrological cycle *Theor. Appl. Climatol.* **136** 135–44

IPCC 2013 Climate change 2013: the physical science basis *Contribution of Working Group I to the Fifth Assessment Report of the Intergovernmental Panel on Climate Change* (Cambridge: Cambridge University Press) p 1535

Jacob D *et al* 2014 EURO-CORDEX: new high-resolution climate change projections for European impact research *Reg. Environ. Change* **14** 563–78

Keenan T F, Hollinger D Y, Bohrer G, Dragoni D, Munger J W, Schmid H P and Richardson A D 2013 Increase in forest water-use efficiency as atmospheric carbon dioxide concentrations rise *Nature* **499** 324

Kjellström E *et al* 2018 European climate change at global mean temperature increases of 1.5 °C and 2 °C above pre-industrial conditions as simulated by the EURO-CORDEX regional climate models *Earth Syst. Dyn.* **9** 459–78

Kotlarski S *et al* 2014 Regional climate modeling on European scales: a joint standard evaluation of the EURO-CORDEX RCM ensemble *Geosci. Model Dev.* **7** 1297–333

Lemordant L and Gentine P 2019 Vegetation response to rising CO_2 impacts extreme temperatures *Geophys. Res. Lett.* **46** 1383–92

Lemordant L, Gentine P, Swann A S, Cook B I and Scheff J 2018 Critical impact of vegetation physiology on the continental hydrologic cycle in response to increasing CO_2 *Proc. Natl Acad. Sci.* **115** 4093–8

Lowe J A *et al* 2018 UKCP18 science overview report *Tech. Rep.* Met Office

Miralles D G, Teuling A J, van Heerwaarden C C and de Arellano J V-G 2014 Mega-heatwave temperatures due to combined soil desiccation and atmospheric heat accumulation *Nat. Geosci.* **7** 345–9

Morison J I L 1985 Sensitivity of stomata and water use efficiency to high CO_2 *Plant, Cell Environ.* **8** 467–74

Nabat P, Kiki S S, Mallet M and Michou M 2016 Impact of aerosols in regional climate projections over the Mediterranean area *Air Pollution Modeling and its Application XXIV* ed D G Steyn and N Chaumerliac (Berlin: Springer) pp 73–8

Oleson K W 2010 Technical description of version 4.0 of the Community Land Model (CLM) *Tech. Rep.* NCAR/TN-478 +STR NCAR (https://doi.org/10.5065/D6FB50WZ)

Perkins S E 2015 A review on the scientific understanding of heatwaves–Their measurement, driving mechanisms, and changes at the global scale *Atmos. Res.* **164–165** 242–67

Reyes-Fox M, Steltzer H, Trlica M, McMaster G S, Andales A A, LeCain D R and Morgan J A 2014 Elevated CO_2 further lengthens growing season under warming conditions *Nature* **510** 259

Riahi K *et al* 2011 RCP 8.5-A scenario of comparatively high greenhouse gas emissions *Clim. Change* **109** 33–57

Roeckner E 1996 The atmospheric general circulation model ECHAM-4: Model description and simulation of present day climate *Tech. Rep.* MPI-Report No. 218 MPI für Meteorologie, Hamburg

Roeckner E 2003 The atmospheric general circulation model ECHAM 5. part I: Model description *Tech. Rep.* MPI-Report No. 349 MPI für Meteorologie, Hamburg

Rummukainen M 2016 Added value in regional climate modeling *Wiley Interdiscip. Rev. Clim. Change* **7** 145–59

Samuelsson P, Gollvik S, Kupiainen M, Kourzeneva E and van de Berg W J 2015 The surface processes of the Rossby Centre regional atmospheric climate model (RCA4) SMHI 157 (http://smhi.se/polopoly_fs/1.89799!/Menu/general/extGroup/attachmentColHold/mainCol1/file/meteorologi_157.pdf)

Schulz J-P, Dümenil L and Polcher J 2001 On the land surface-atmosphere coupling and its impact in a single-column atmospheric model *J. Appl. Meteorol.* **40** 642–63

Sellers P *et al* 1997 Modeling the exchanges of energy, water, and carbon between continents and the atmosphere *Science* **275** 502–9

Seneviratne S I *et al* 2012 Changes in climate extremes and their impacts on the natural physical environment *Managing the Risks of Extreme Events and Disasters to Advance Climate Change Adaptation. A Special Report of Working Groups I and II of the Intergovernmental Panel on Climate Change (IPCC)* ed C B Field *et al* (Cambridge: Cambridge University Press) pp 109–230

Seneviratne S I, Corti T, Davin E L, Hirschi M, Jaeger E B, Lehner I, Orlowsky B and Teuling A J 2010 Investigating soil moisture-climate interactions in a changing climate: A review *Earth Sci. Rev.* **99** 125–61

Skinner C B, Poulsen C J and Mankin J S 2018 Amplification of heat extremes by plant CO_2 physiological forcing *Nat. Commun.* **9** 1094

Sørland S L, Schär C, Lüthi D and Kjellström E 2018 Bias patterns and climate change signals in GCM-RCM model chains *Environ. Res. Lett.* **13** 074017

Swann A L S, Hoffman F M, Koven C D and Randerson J T 2016 Plant responses to increasing CO_2 reduce estimates of climate impacts on drought severity *Proc. Natl Acad. Sci.* **113** 10019–24

Ukkola A M, Prentice I C, Keenan T F, van Dijk A I, Viney N R, Myneni R B and Bi J 2016 Reduced streamflow in water-stressed climates consistent with CO_2 effects on vegetation *Nat. Clim. Change* **6** 75

Vogel M M, Zscheischler J and Seneviratne S I 2018 Varying soil moisture-atmosphere feedbacks explain divergent temperature extremes and precipitation projections in central Europe *Earth Syst. Dyn.* **9** 1107–25

Westervelt D M, Horowitz L W, Naik V, Golaz J-C and Mauzerall D L 2015 Radiative forcing and climate response to projected 21st century aerosol decreases *Atmos. Chem. Phys.* **15** 12681–703

White P W 2001 IFS documentation part IV: physical processes (CY23R4) *Tech. Rep.* 4 ECMWF